Prodan Fluorescence Reflects Differences in Nucleotide-Induced Conformational States in the Myosin Head and Allows Continuous Visualization of the ATPase Reactions†

Toshiaki Hiratsuka*

Department of Chemistry, Asahikawa Medical College, Asahikawa, Hokkaido 078, Japan

Received December 15, 1997; Revised Manuscript Received March 3, 1998

ABSTRACT: The noncovalent fluorescent probe 6-propionyl-2-(dimethylamino)naphthalene (prodan) binds stoichiometrically to myosin subfragment-1 (S-1) without affecting the ATPase and actin-binding properties of S-1. Neither ATP nor actin interferes with the prodan binding. Free prodan exhibits a green emission peak at 520 nm. However, the prodan bound to S-1 and the S-1·ADP complex shows blue emission peaks at 460 and 450 nm, respectively, which allow easy separation of the fluorescence contributions from the free and bound probes. In the S-1**·ADP·P_i state, the blue emission peak is further shifted to 445 nm with a large (4.5-fold) fluorescence enhancement. Thus, prodan in the presence of S-1 exhibits predominantly blue fluorescence only during ATP hydrolysis, and so visualizes the ATPase reaction continuously. The initial velocities of the steady state of the Mg^{2+}-, Ca^{2+}-, and actin-activated ATPases can be conveniently calculated from the blue fluorescence changes. The ability of different nucleoside triphosphates (NTP) to enhance the blue fluorescence of prodan follows the order ATP > CTP > UTP > ITP > GTP. This order agrees with those of the extent of hydrophobicity near the ribose of the corresponding nucleoside diphosphates (NDP) trapped to S-1 with orthovanadate (V_i) [Hiratsuka, T. (1984) *J. Biochem. (Tokyo) 96,* 155−162] and the ability of different NTPs to support force production in muscle fibers [Regnier, M., et al. (1993) *Biophys. J. 64,* A250]. The rate of formation of the corresponding S-1·NDP·V_i complex also follows this order, whereas the NTPase rate follows the reverse order. These results indicate that nucleotide-induced changes in prodan fluorescence correspond to the nucleotide-induced conformational states of S-1. Thus, the use of prodan in studies of the myosin ATPase offers a new and promising approach not only to monitoring the ATPase reaction but also to investigating the structural changes during ATP hydrolysis.

Most nonpolar groups in proteins are buried in the interior of the protein molecule. However, some are found in clefts or pockets in the molecule. These may form hydrophobic sites of interaction with small effector molecules, especially hydrophobic compounds, including various drugs, dyes, and fluorescent probes. Such sites may also become exposed as a result of biologically significant conformational changes of protein molecules. Indeed, hydrophobic sites in various enzymes often sense the conformational changes that occur in the active sites even if these two sites are distant from each other (*1*−*5*). Thus, fluorescent probes that bind stoichiometrically to hydrophobic sites in enzymes and reflect the conformational changes in the active sites should greatly facilitate further studies on the structure−function relationship of enzymes.

The fluorescent probes having an aminonaphthalene structure such as 1,8-anilinonaphthalenesulfonate (ANS)[1] and the dimer bis(1,8-anilinonaphthalenesulfonate) (bisANS) are fluorescent probes whose fluorescence is greatly increased in media with low dielectric constants and are widely used as sensitive reporters for hydrophobic sites of proteins, including myosin and myosin subfragment-1 (S-1) (*6*−*8*). On the other hand, another aminonaphthalene, 2-(*p*-toluidinyl)naphthalene-6-sulfonate (TNS), has been used as a fluorescent probe for Ile-tRNA synthetase (*2*, *9*). Binding of the probe to the enzyme interferes with neither substrate binding nor the enzyme action. Furthermore, the binding properties of TNS are scarcely altered by various substrates. However, the formation of binary and ternary enzyme−substrate complexes is accompanied by a significant change in the TNS fluorescence. Thus, the reaction between the enzyme and substrates is reflected by a large change in fluorescence of the enzyme-bound TNS as if this would be an intrinsic property of the enzyme. Properties of interaction between the enzyme and various ligands are conveniently evaluated from changes in TNS fluorescence without including consideration of the enzyme−TNS interaction.

† This study was supported in part by a Grant-in-Aid for Scientific Research on Priority Areas 09279202 from the Ministry of Education, Science, Sports and Culture of Japan and by a Research Grant from Yazaki Memorial Foundation for Science and Technology.

* Corresponding author. Telephone and Fax: 0166-66-0123. E-mail: toshiaki@asahikawa-med.ac.jp.

[1] Abbreviations: S-1, myosin subfragment-1; prodan, 6-propionyl-2-(dimethylamino)naphthalene; ANS, 1,8-anilinonaphthalenesulfonate; bisANS, bis(1,8-anilinonaphthalenesulfonate); TNS, 2-(*p*-toluidinyl)-naphthalene-6-sulfonate; HEPES, 4-(2-hydroxyethyl)-1-piperazineethanesulfonic acid; DMF, *N*,*N*-dimethylformamide; V_i, orthovanadate; AMP-PNP, adenyl-5′-yl imidodiphosphate; NTP, nucleoside triphosphate; NDP, nucleoside diphosphate; Mant, 2′(3′)-*O*-(*N*-methylanthraniloyl).

S0006-2960(97)03083-3 CCC: $15.00
Published on Web 04/28/1998

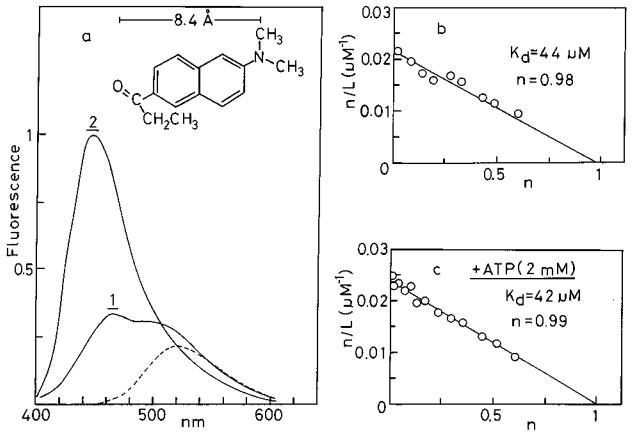

FIGURE 1: Binding of prodan to S-1 in the presence and absence of ATP. (a) Fluorescence spectra of prodan (1 μM) in the presence and absence of S-1 (64 μM) were measured in buffer A at 25 °C: - - -, free prodan; curve 1, prodan and S-1; and curve 2, prodan, S-1, and ATP (2 mM). Samples were excited at 360 nm. The inset shows the structure of prodan. (b and c) Scatchard plots of prodan binding to S-1 in the presence (c) and absence (b) of ATP (2 mM). The fluorescence increase of prodan (1 μM) was measured at 460 nm (b) and 445 nm (c) in the presence of varying amounts of S-1 (0.5−64 μM). The dissociation constant and number of prodan binding sites on S-1 for the complex were calculated by Scatchard analysis as described previously (*19*). *n* is the moles of prodan bound per mole of S-1. *L* is the concentration of free S-1.

The X-ray crystallographic structure of S-1 reveals some clefts and pockets on the protein (*10*). The presence of a hydrophobic pocket on S-1 where various noncovalent fluorophores stoichiometrically bind was proposed some time ago (*11*). I have initiated a study of noncovalent fluorophores that bind to a hydrophobic pocket on S-1 and display large spectral shifts to visualize the ATP hydrolysis reaction. Several noncovalent fluorescent probes (more than 40) were examined in an attempt to incorporate one into a hydrophobic pocket on S-1 that senses differences in the nucleotide-induced conformational states of the ATP binding pocket. Of the probes tested, 6-propionyl-2-(dimethylamino)naphthalene (prodan, Figure 1a inset) was chosen as a fluorescent probe for S-1. The absence of a charge and an extreme sensitivity of its emission spectrum to changes in environmental polarity make prodan a more attractive fluorescent probe than ANS and bisANS (*12*). Although prodan has successfully been used in some studies with apomyoglobin (*13*), tubulin (*14*), and spectrin (*15*), no study has been reported on its interaction not only with myosin but also with S-1.

In this work, I have studied the interaction of prodan with S-1. The data provide evidence for the existence of a single site in S-1 that is bound by prodan and is very sensitive to the conformational states of the ATP binding pocket. Neither ATP nor actin interferes with the prodan binding. Prodan itself has little effect on the ATPase and actin-binding properties of S-1. Thus, the bound prodan behaves well as if it would be an intrinsic fluorophore of S-1. The fluorescent properties of prodan enable me to isolate the S-1 in the S-1**·ADP·P_i state from the others in the free and S-1*·ADP states and visualize the ATPase reactions continuously. Thus, the initial velocities of the steady state of the ATPases in the presence and absence of actin can be determined directly from changes in the fluorescence of prodan. Furthermore, the extent of nucleotide-induced enhancement of prodan fluorescence serves as an index not only of conformational changes in the ATP binding pocket but also of force production in muscle fibers. Therefore, prodan should greatly facilitate further studies of the ATPase mechanism of actomyosin.

MATERIALS AND METHODS

Materials. Prodan was purchased from Molecular Probes. TLC (Silica Gel 60 F_{254}) plates were from Merck. AMP-PNP was from Sigma. NTPs and NDPs were from Yamasa Co. V_2O_5 was from Nakarai Chemical Co. Stock solutions of V_i were prepared as described by Goodno (*16*). Other reagents were of reagent or biochemical research grade.

Purity Check of Prodan. Purity was checked by TLC on silica plates (Silica Gel 60 F_{254}) in 1-butanol/1 M acetic acid (9:1, $R_f = 0.88$), chloroform/methanol (95:5, $R_f = 0.85$), and acetone/water (1:1, $R_f = 0.88$). In no case could another fluorescent or UV-absorbing compound be detected. Prodan concentrations in DMF were determined using a molar absorption coefficient of 18 000 M^{-1} cm^{-1} at 360 nm (*12*), which agreed well with those calculated from weight determinations. Prodan was added to 1−6 μM from 0.5−12 mM stock solutions in DMF or dimethyl sulfoxide.

Protein Preparation. S-1 (*17*) and actin (*18*) were prepared from rabbit skeletal muscle, and the protein concentrations were determined from the absorbance at 280 nm as in my previous works (*19, 20*).

Buffer Systems. All experiments with protein samples were carried out at 25 °C in the following buffers: buffer A [25 mM HEPES (pH 8.0), 30 mM KCl, and 2 mM $MgCl_2$] and buffer B [50 mM HEPES (pH 8.0), 60 mM KCl, and 2 mM $CaCl_2$]. Since prodan was scarcely soluble in water (*12*), all mixtures for experiments with the probe contained 0.2% DMF or dimethyl sulfoxide. The addition of 0.2% organic solvents had no effect on all ATPases of S-1 regardless of the presence and absence of actin. There was no difference between DMF and dimethyl sulfoxide in the results of measurements for the prodan binding and kinetics of the ATPases of S-1.

Spectral Measurements. Absorption spectra were measured at room temperature with a Shimadzu MPS-2000 spectrophotometer. Uncorrected fluorescence emission spectra were recorded at 25 °C in a thermostated Hitachi fluorescence spectrophotometer (model F-4010). The slit widths on excitation and emission monochromators were 5 nm. Excitation wavelengths were 290 nm (Trp fluorescence) and 360 nm (prodan fluorescence).

Prodan Binding Measurements. Dissociation constants for the prodan complexes and the number of prodan binding sites on S-1 and acto-S-1 were determined at 25 °C in buffer A as follows. The fluorescence of prodan (1 μM) was measured at 460 nm in the presence and absence of S-1 at various concentrations (0.5−64 μM). In the presence of ATP (2 mM), the fluorescence was measured at 445 nm during the steady state of ATP hydrolysis. For measurements of acto-S-1, the protein was prepared from S-1 using a 1.5-fold molar excess of actin. The amount of bound prodan was calculated from the fluorescence increase due to probe binding. The dissociation constant and the number of prodan binding sites on proteins were calculated by Scatchard analysis as described previously (*19*).

ATPase Measurements. The initial velocities of steady state of the ATPases of S-1 (k_{cat}) were measured at 25 °C. That of Mg^{2+}-ATPase was measured in buffer A using 0.1−1 mM ATP and 1 μM S-1. That of Ca^{2+}-ATPase was measured in buffer B using 2 mM ATP and 0.1 μM S-1. That of actin-activated Mg^{2+}-ATPase was measured in buffer A using 1 mM ATP and 0.5 μM S-1 at various concentrations of actin (2.5−20 μM). Liberated P_i was determined by the method of Fiske and SubbaRow (*21*).

Kinetic Measurements. For the measurements of the NTP-induced changes in fluorescence of prodan and Trp, S-1 or acto-S-1 in the presence and absence of prodan was preincubated at 25 °C. Kinetics were followed by observing the time-dependent fluorescence change after rapid mixing with an aliquot of NTP. Fluorescence of prodan was monitored at 445 nm with excitation at 360 nm. Trp fluorescence was monitored at 340 nm with excitation at 290 nm. The measurements were carried out with NTP at concentrations that made it an at least 18-fold molar excess over S-1. Concentrations of NTP and S-1 used were 1 μM to 4 mM and 42 nM to 11 μM, respectively. For acto-S-1, the measurements were carried out with a fixed amount of S-1 (0.5 μM) in the presence of actin at various concentrations (2.7−38 μM).

Treatment of the Kinetic Data. Since the ATPase reaction catalyzed by myosin obeys the simple Michaelis−Menten relationship (eq 1)

$$\mathrm{E} + \mathrm{S} \underset{k_{-1}}{\overset{k_1}{\rightleftharpoons}} \mathrm{ES} \xrightarrow{k_2} \mathrm{E} + \mathrm{P} \qquad (1)$$

Morita (*22*) has demonstrated that a rate constant, k_2, for the decay of the intermediate complex (ES) of heavy meromyosin and ATP can be adequately approximated from the ATP-induced absorbance change of Trp residues according to an equation (eq 2) derived by Chance (*23*)

$$k_2 = \frac{s_0}{e_0 \tau} \qquad (2)$$

provided a sufficiently high concentration of ATP is used. In eq 2, s_0 and e_0 are initial concentrations of ATP and the enzyme, respectively, and τ is the time required for the decay of absorbance to occur by one-half of its maximum amplitude. The k_2 values calculated using eq 2 agree well with the initial velocities of the steady state of the ATPase, k_{cat}, provided a molar excess of ATP over the enzyme of at least 15-fold is used (*22*). In this work, the ATP-induced change of Trp fluorescence (*24*) instead of the absorbance was measured with S-1, and the rate constant (k_2) was calculated using eq 2.

When the noncovalent fluorescent probe prodan is added to S-1, the bound probe behaves like an intrinsic fluorophore of S-1, i.e., ATP-sensitive Trp residues (see Results). Thus, the rate constant (k_2) may be calculated from the NTP-induced change in the prodan fluorescence using eq 2. Indeed, an observed ATP-induced fluorescence enhancement (ΔF) at 445 nm in the presence of 4 μM prodan was proportional to the concentration of the complex of S-1 with ATP with a wide range of S-1 concentrations (0.04−11 μM). Thus, considerations similar to those used in dealing with changes in absorbance of Trp (*22*) can be applied without including consideration of the interaction between S-1 and prodan.

RESULTS

Binding of Prodan to S-1. The structure of prodan is given in the inset of Figure 1a. Upon excitation at 360 nm, prodan shows significant fluorescence in the range of 460−600 nm. Figure 1a shows the emission spectra of free prodan in buffer A and the prodan bound to S-1. The free prodan exhibits an emission maximum at 520 nm (*12*), while there is a significant increase in the fluorescence intensity at 460 nm upon formation of the prodan·S-1 complex. However, the fluorescence spectrum of the prodan·S-1 complex in the presence of ATP was quite different from that of the complex alone. Upon addition of a large excess of ATP (2 mM), the emission maximum at 460 nm is further blue-shifted to 445 nm, which is accompanied by a 4.5-fold increase in the fluorescence intensity at 445 nm. Since the fluorescence measurements were completed within 2 min, the spectrum obtained with ATP was regarded as the spectrum during the steady state of ATP hydrolysis. It should be emphasized that the coexistent unbound prodan scarcely contributes to fluorescence of the complex at 445−460 nm since the intensity for the unbound is less than 3% of those observed with the complexes in the presence and absence of ATP.

The changes in fluorescence of prodan induced by the binding to S-1 allow titration of the probe with S-1 in the presence and absence ATP. The shape of the titration curve was hyperbolic in both cases (not shown). A dissociation constant for the prodan·S-1 complex and the number of prodan binding sites were calculated by Scatchard analysis. The data yielded linear plots in both cases. The number of prodan binding sites was found to be 0.98 mol/mol of S-1 with a dissociation constant of 44 μM (Figure 1b). ATP scarcely affects the binding of prodan to S-1, yielding a number of prodan binding sites of 0.99 mol/mol of S-1 with a dissociation constant of 42 μM during the steady state of ATP hydrolysis (Figure 1c). These results suggest that prodan and ATP do not compete for the same site in S-1.

Fluorescence Spectra of the Prodan·S-1 Complex in the Presence of Other Nucleotides. The fluorescence spectra of the prodan·S-1 complex in the presence of various nucleotides and the analogue were also measured. As shown in Figure 2a, the fluorescence spectra of the prodan·S-1 complex in the presence of ATP, AMP-PNP, and ADP·V_i are similar, exhibiting an emission maximum at 445 nm. However, the spectrum obtained in the presence of ADP is different from the others, showing an emission maximum at 450 nm. This spectrum was rather similar to that of the prodan·S-1 complex (Figure 1a). Fluorescence intensities at 445 nm observed for the complexes in the presence of ADP, AMP-PNP, and ADP·V_i were 21, 51, and 59% of the intensity observed for the complex in the presence of ATP, respectively. These results suggest that the prodan bound to S-1 reflects differences in conformation between various states of the ATP binding pocket which are induced by nucleotides and the analogue.

The rate of formation of the ternary complex of S-1 with ADP and V_i is conveniently measured from an increase in prodan fluorescence. In a typical experiment, V_i (1.2 mM)

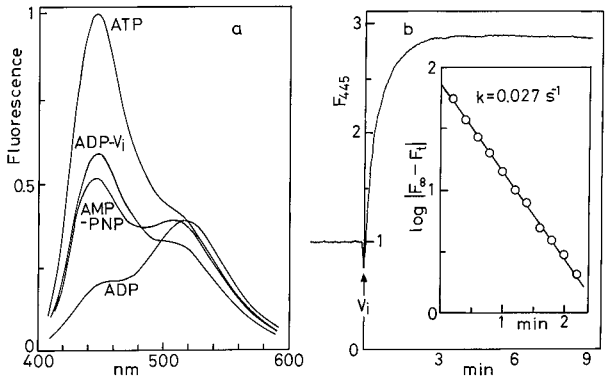

FIGURE 2: Changes in fluorescence emission spectrum of the prodans·S-1 complex induced by ADP, AMP-PNP, ADP·V_i, and ATP. (a) Fluorescence spectra of the complex of S-1 (21 μM) with prodan (4 μM) were recorded in the presence of various ligands (1 mM nucleotides and 1.2 mM V_i). (b) Formation of the ternary complex between ADP·S-1 and V_i monitored by prodan fluorescence. ADP (1 mM) was initially mixed with S-1 (21 μM) in the presence of prodan (4 μM) in buffer A at 25 °C. After completion of the binding reaction, ternary complex formation was initiated by the addition of 1.2 mM V_i, monitored at 445 nm with excitation at 360 nm. The inset shows a semilog plot of the V_i-induced fluorescence change against time; data were taken from panel b.

was added to S-1 (21 μM) in the presence of ADP (1 mM) and prodan (4 μM), and then fluorescence was monitored (Figure 2b). The final fluorescence intensity was 290% of the original value. The time course fitted an exponential profile yielding a rate constant of 0.027 s^{-1} (inset). This rate constant is lower than the corresponding value (0.05 s^{-1}) that is measured at pH 7.0 (*25*). Taking into account the fact that the rate of formation of the ternary complex of myosin with ADP and V_i is faster at lower pH (*25*), this result suggests that S-1 in the presence of prodan forms the ternary complex with ADP and V_i at a rate similar to that of S-1 alone.

Fluorescence Visualization of ATP Hydrolysis Reactions. The result shown in Figure 2a indicates that the fluorescence intensity at 445 nm of the prodan bound to S-1 increases significantly during ATP hydrolysis. This raises the possibility that the ATP hydrolysis reaction would be visualized by taking advantage of such a large fluorescence enhancement of the bound prodan. Thus, the ATP-induced changes in the fluorescence spectrum of prodan in the presence of S-1 were followed as a function of time.

When a large excess of ATP (2 mM) was added to S-1 (20 μM) in the presence of prodan (1 μM) at time 0 (Figure 3a), the fluorescence spectrum was converted rapidly into that with an increased emission at 445 nm (Figure 3b). When ATP was exhausted, the fluorescence intensity at 445 nm reverted to the original level (Figure 3c). This final spectrum was essentially identical to that of the prodan·S-1 complex in the presence of ADP (- - -).

Alternatively, the ATP-induced fluorescence changes of the reaction mixtures may be expressed by changes in the intensity ratio of the blue fluorescence peak for the bound prodan (F_{445}) to the green fluorescence peak for the coexistent unbound (F_{520}). As indicated in Figure 3, the ratio F_{445}/F_{520} was changed from 0.47 to 2.6 upon the addition of ATP (panel b). However, when ATP was exhausted, the value fell to 0.57 (panel c). This value was similar to that (0.47) obtained before the addition of ATP (panel a). Thus, only during ATP hydrolysis, the blue fluorescence becomes

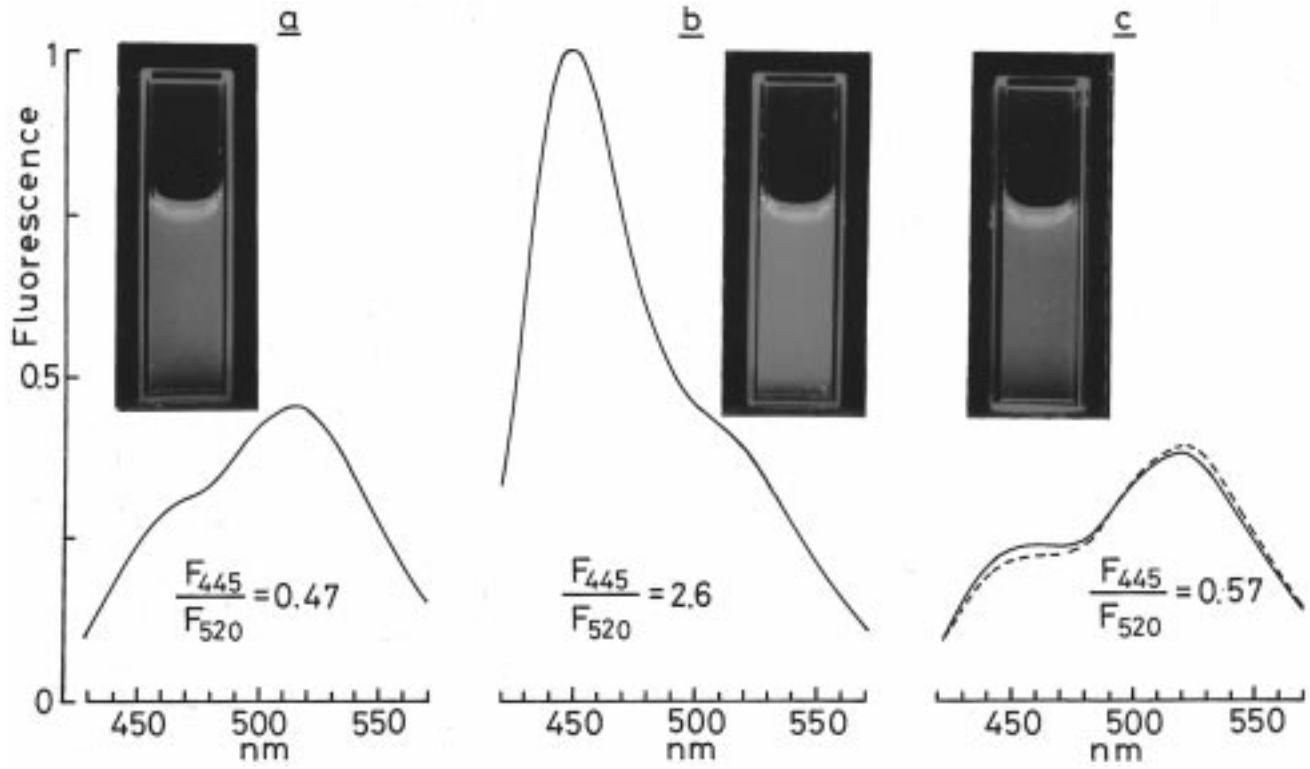

FIGURE 3: Fluorescence visualization of the ATP hydrolysis reaction of S-1 by prodan. Fluorescence spectra were measured for the complex of S-1 (20 μM) with prodan (1 μM) at appropriate time intervals after mixing with ATP (2 mM): (a) 0 min, (b) 5 min, (c) 45 min, and (- - -) the complex of S-1 (20 μM) with prodan (1 μM) in the presence of ADP (2 mM). Other conditions are described in the legend of Figure 1. (Inset) In a separate experiment, fluorescence photographs of the reaction mixtures were taken under UV irradiation in a dark room under the same conditions as described above.

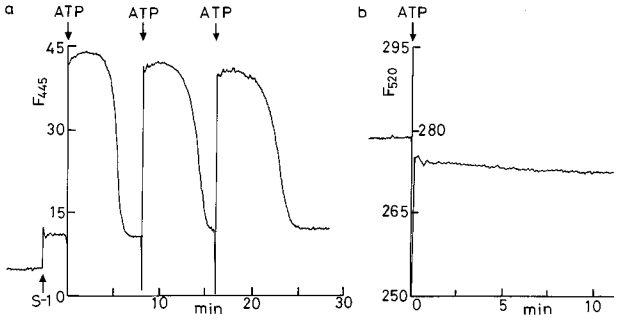

FIGURE 4: Time courses of the ATP-induced changes in fluorescence of the prodan·S-1 complex monitored at 445 nm (a) and 520 nm (b). (a) At time 0, ATP (20 μM) was added to the complex of S-1 (1.1 μM) with prodan (4 μM), and fluorescence was measured at 445 nm. Upon exhaustion of ATP, one more amount of ATP (20 μM) was added to the same reaction mixture and fluorescence was recorded again. It was repeated once again. (b) Fluorescence was measured at 520 nm under the same condition as described in panel a. Other conditions are described in the legend of Figure 1.

dominant. On the other hand, the green fluorescence derived from the unbound prodan is dominant before and after ATP hydrolysis. Fluorescence photographs of the reaction mixtures, which were taken in a dark room at appropriate time intervals during the course of ATP hydrolysis, reveal such dramatic changes in the color of fluorescence (Figure 3 insets).

To confirm this point further, the ATP-induced change in the fluorescence intensity at 445 nm was followed as a function of time. Since the addition of prodan ranging in concentration from 1 to 6 μM had no effect on the Mg^{2+}-ATPase of S-1 (not shown), the fluorescence intensity at 445 nm was monitored in the presence of 4 μM prodan. As shown in Figure 4a, the fluorescence intensity increased rapidly to 2.3-fold when S-1 was added to solutions of prodan alone. The binding of prodan to S-1 was rapid, being completed within a mixing time of about 5 s. No further fluorescence change was observed thereafter. Addition of ATP to the prodan·S-1 complex further caused a 4.3-fold fluorescence enhancement. This fluorescence level was maintained for a while and then began to decay gradually. The fluorescence intensity after the decay was similar to the original value.

It should be emphasized that changes in the blue fluorescence can be reproduced by further addition of ATP to the reaction mixtures where the initial changes have been over. This indicates that prodan causes neither the interference with the action of S-1 in the turnover reaction of ATP hydrolysis nor the irreversible denaturation of S-1. On the other hand, a decrease of only 1−2% in the fluorescence intensity at 520 nm was observed upon the addition of ATP (Figure 4b). The intensity remained unchanged even when ATP was exhausted. This suggests that the free prodan remains uunbound even when ATP is exhausted. Thus, the ATP-induced fluorescence change originates solely from the S-1 bound by prodan, as if this would be an intrinsic property of S-1.

Kinetic Analysis of ATP-Induced Changes in Prodan Fluorescence. It has been established that the ATP hydrolysis rate of the myosin ATPase can be conveniently calculated from the ATP-induced absorption changes of Trp residues (*22*), provided a sufficiently high concentration of ATP is used. This method is based on the determination of a rate

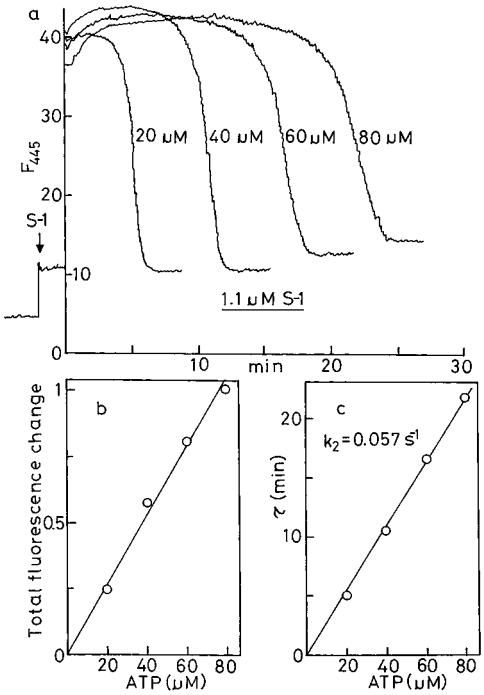

FIGURE 5: Kinetic analysis of ATP-induced changes in fluorescence of the prodan·S-1 complex in the presence of Mg^{2+}. (a) At time 0, varying amounts of ATP (20−80 μM) were added to the complex of S-1 (1.1 μM) with prodan (4 μM) and fluorescence was recorded at 445 nm. Other conditions are described in the legend of Figure 1. (b) Relationship between the total fluorescence change and ATP concentration. The total fluorescence change is defined as the integrated area between the fluorescence decay curve and the baseline obtained at the end, taken from the data shown in Figure 5a. The total fluorescence change is expressed relative to the area obtained with 80 μM ATP. (c) Relationship between ATP concentration and a value of τ, the time required for the fluorescence decay to occur by one-half of its maximum amplitude. Data were taken from panel a. A rate constant (k_2) for the decay of fluorescence was calculated according to an equation derived by Chance (*23*) (see Materials and Methods).

constant (k_2) for the breakdown of the intermediate complexes of the enzyme with ATP using an equation derived by Chance (*23*). These results raise the possibility that ATP-induced change in the prodan fluorescence can also be applied to the calculation of the ATPase rate. Next, I checked whether such a kinetic analysis is valid or not in this case.

Figure 5a shows time courses of the ATP-induced changes in fluorescence of the prodan bound to S-1 in buffer A using various concentrations of ATP (20−80 μM). The addition of ATP to the prodan·S-1 complex results in an initial increase of prodan fluorescence with a subsequent decay of the fluorescence as described above. When the area between the fluorescence decay curve and the baseline obtained at the end, which is the total fluorescence intensity changes during the whole time course of the ATP hydrolysis reaction, was plotted against the initial concentration of ATP added, a linear relationship was obtained (Figure 5b). Furthermore, a value of τ, the time required for the fluorescence decay to occur by one-half of its maximum amplitude, was also proportional to the initial concentration of ATP added (Figure 5c). Although data are not shown, the extent of fluorescence enhancement in the presence of saturating amounts of ATP was also proportional to the initial concentration of S-1 used in the range of 0.04−11 μM, suggesting that the observed

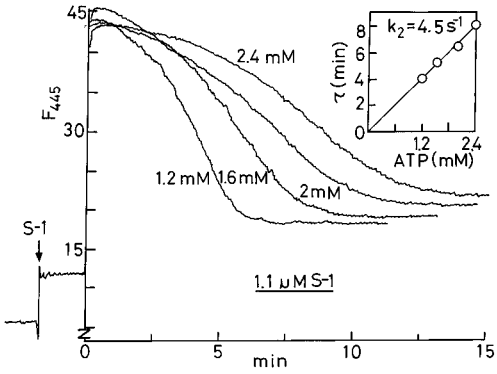

FIGURE 6: Time courses of the ATP-induced changes in fluorescence of the prodan·S-1 complex in the presence of Ca^{2+}. At time 0, varying amounts of ATP (1.2−2.4 mM) were added to the complex of S-1 (1.1 μM) with prodan (4 μM) in buffer B at 25 °C. Fluorescence was measured at 445 nm with excitation at 360 nm. The inset shows the relationship between ATP concentration and a value of τ. A rate constant (k_2) for the decay of fluorescence was calculated as described in the legend of Figure 5.

fluorescence change at 445 nm (ΔF) is proportional to the concentration of a nucleotide·S-1 complex. From these results, one may conclude that the ATP-induced change in fluorescence of the prodan bound to S-1 reveals two elementary steps in the ATP hydrolysis reaction, i.e., the formation and breakdown of intermediate complexes (*22*, *23*, *26*). Thus, the decay curve of the prodan fluorescence reveals the breakdown of the intermediate complexes of S-1 with ATP (S-1**·ADP·P_i), as if the prodan bound to S-1 would be the ATP-sensitive Trp residues of S-1 (*22*, *24*). The mean value for k_2 was calculated to be 0.057 s^{-1} (see Materials and Methods).

The ATP-induced change in the prodan fluorescence could be detected using very small amounts of S-1 (not shown). Upon addition of ATP (1−3 μM) to S-1 (42 nM), the enhancement of the prodan fluorescence occurred followed by a subsequent decay of the fluorescence similar to the results shown in Figure 5a. Furthermore, the value of τ was proportional to the initial concentration of ATP added, indicating that the kinetic analysis described above is valid even under this condition. The mean value of k_2 was calculated to be 0.078 s^{-1}, which was somewhat higher than the value obtained with larger amounts of S-1 (Figure 5).

The interaction of prodan with S-1 was also examined in the presence of Ca^{2+}. As shown in Figure 6, the binding of prodan to S-1 in the presence of Ca^{2+} was also rapid, as was also true in the presence of Mg^{2+} (Figure 4a). When a large excess of ATP (1.2−2.4 mM) was added to the prodan·S-1 complex, the fluorescence intensity at 445 nm increased rapidly to about 4-fold followed by a subsequent decay of the prodan fluorescence. The value of τ was proportional to the initial concentration of ATP added. Thus, the rate constant (k_2) for the breakdown of the intermediate (S-1**·ADP·P_i) may be calculated from the decay curve of the prodan fluorescence as described above. The mean value for k_2 was calculated to be 4.5 s^{-1}. This value was about 79 times greater than that obtained in the presence of Mg^{2+} (Figure 5c).

Comparison of the Rate Constant Obtained from Prodan Fluorescence Decay and the Initial Velocity of the Steady State of the ATPase. The above results suggest that a rate constant, k_2, obtained from the decay curve of prodan fluorescence may be taken as an initial velocity, k_{cat}, of steady state of ATPase of S-1 as established in the ATP-induced absorption changes of Trp residues (*22*). To confirm this point further, the k_2 values were compared with the k_{cat} values in the presence of Mg^{2+} and Ca^{2+} over a wide range of concentrations of S-1 and ATP. For comparative purposes, the k_2 values obtained from the decay curve of Trp fluorescence under similar conditions are also listed (Table 1).

Table 1: Comparison of k_{cat} and k_2 Values for S-1

			k_2 (s^{-1})	
ATPase	k_{cat} (s^{-1})	condition[b]	prodan	Trp
Mg^{2+}-ATPase		A	0.078 ± 0.01	ND
	0.058 ± 0.002	B	0.069 ± 0.004	0.066 ± 0.007
		C	0.059 ± 0.003	0.061 ± 0.005
		D	0.058 ± 0.002	ND
Ca^{2+}-ATPase	4.8 ± 0.2	E	4.5 ± 0.1	4.9 ± 0.2

[a] For values of k_{cat}, P_i assays were carried out in the absence of prodan according to the method of Fiske and SubbaRow (*21*): Mg^{2+}-ATPase, 1 μM S-1, and 0.1−1 mM ATP; Ca^{2+}-ATPase, 0.1 μM S-1, and 2 mM ATP. Values of k_2 were calculated from the decay of the increased fluorescence of prodan (4 μM) and Trp of S-1 using an equation derived by Chance (*23*) (see Materials and Methods). All measurements were performed at 25 °C in buffer A (Mg^{2+}-ATPase) and buffer B (Ca^{2+}-ATPase). All values are the average and standard deviation of three to eight independent experiments. ND means the value was not determined. [b] (A) [S-1] = 42 nM, and [ATP] = 1−3 μM. (B) [S-1] = 0.1 μM, and [ATP] = 2−4 μM. (C) [S-1] = 0.5−1.1 μM, and [ATP] = 10−100 μM. (D) [S-1] = 11 μM, and [ATP] = 0.4−1.6 mM. (E) [S-1] = 1.1 μM, and [ATP] = 0.8−2.4 mM.

For the Mg^{2+}-ATPase, the k_2 values obtained from the decay curve of prodan fluorescence agree well with those obtained from the decay curve of Trp fluorescence. On the other hand, the k_{cat} value (0.058 s^{-1}) determined from P_i assays agrees well with the k_2 values (0.058−0.059 s^{-1}) when higher concentrations of S-1 (0.5−11 μM) are used. In the case of the use of very small amounts of S-1 (0.04−0.1 μM), the k_2 values obtained (0.069−0.078 s^{-1}) were about 1.2−1.3 times greater than the k_{cat} value. For the Ca^{2+}-ATPase, the k_2 value (4.5 s^{-1}) was similar to the k_{cat} value (4.8 s^{-1}). These values were also similar to the k_2 value (4.9 s^{-1}) obtained from changes in Trp fluorescence of S-1 in the absence of prodan. Thus, it is concluded that a rate constant obtained from the ATP-induced decay curve of prodan fluorescence may be taken as an initial velocity of the steady state of the myosin ATPase when the measurements are performed under conditions where concentrations of ATP are at least 18 times higher than those of S-1.

In the absence of divalent metal ions, the ATP-induced increase and decay of fluorescence were not observed, although a fluorescence increase occurred upon the addition of S-1 to prodan (not shown) as well as in the presence of Mg^{2+} and Ca^{2+} (Figures 5a and 6). Thus, the K^+-EDTA-ATPase of S-1 is unable to be measured by this method.

ATP-Induced Changes in Fluorescence of Prodan Bound to Acto-S-1. The binding of prodan to acto-S-1 was also examined (not shown). The fluorescence spectrum of the complex of prodan with acto-S-1 was similar to that of the prodan·S-1 complex, exhibiting an increase in fluorescence intensity at 460 nm. The Scatchard plot yielded a number of the binding sites (1.1 mol/mol of S-1) and a dissociation constant (30 μM) similar to those obtained with the

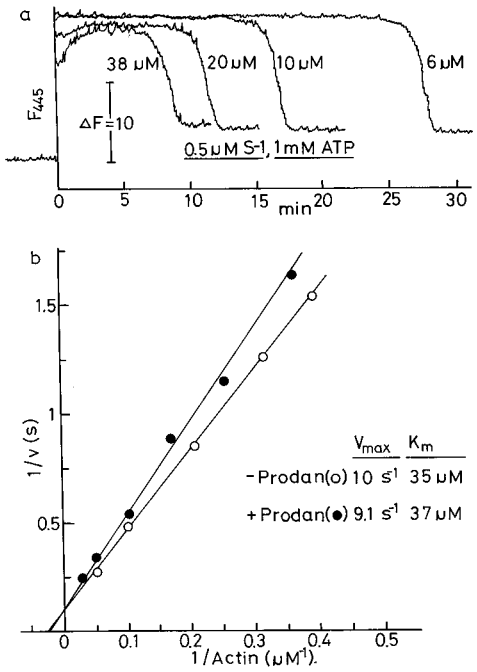

FIGURE 7: Interaction of actin with S-1 in the presence of prodan. (a) Time courses of ATP-induced fluorescence changes were measured for the complex of S-1 (0.5 μM) with prodan (4 μM) in the presence of varying amounts of actin (6−38 μM). At time 0, ATP (1 mM) was added to the complex. Other conditions are described in the legend of Figure 1. (b) Double-reciplocal plots of the ATPase rate against actin concentration were obtained in the presence (●) and absence (○) of prodan. (●) Fluorescence was measured under the same conditions as described in panel a using varying amounts of actin (2.5−38 μM); rate constants (k_2) for the decay of prodan fluorescence were taken as the initial velocities of the steady state of ATPase (k_{cat}) (see Table 1); (○) ATPase rates were measured at 25 °C in buffer A with varying amounts of actin (2.5−20 μM) and 1 mM ATP. P_i liberated was determined by the method of Fiske and SubbaRow (*21*).

prodan·S-1 complex (Figure 1b). Thus, actin scarcely interferes with the binding of prodan to S-1.

The ATP-induced changes in fluorescence of the prodan bound to S-1 were also followed in the presence of actin (not shown). When acto-S-1 was added to prodan, the fluorescence intensity at 445 nm increased rapidly. The extent of ATP-induced fluorescence enhancement obtained with the acto-S-1 complex was similar to that of the enhancement obtained with the S-1 complex. However, a subsequent fluorescence decay of the acto-S-1 complex occurred much more rapidly than that of the S-1 complex (see below).

Interaction of Actin with S-1 in the Presence of Prodan. Figure 7a shows time courses of the ATP-induced changes in fluorescence of the prodan bound to S-1 in the presence of varying amounts of actin. When a large excess of ATP (1 mM) was added to S-1 (0.5 μM) in the presence of varying amounts of actin, the extent of ATP-induced fluorescence enhancement of prodan (4 μM) was similar regardless of the concentrations of actin. This suggests that even in acto-S-1 the ATP-induced change in prodan fluorescence originates solely from conformational changes of S-1. On the other hand, the value of τ, the time required for the fluorescence decay to occur by one-half of its maximum amplitude, was gradually decreased from 27.4 to 8.3 min by changing the concentration of actin from 6 to 38 μM. These results confirm that even in the presence of actin the ATP-induced enhancement and decay of prodan fluorescence reflect the formation and breakdown of the intermediate complexes of acto-S-1 with ATP, respectively. Thus, a rate constant k_2 obtained from the decay curve of prodan fluorescence may be taken as an initial velocity of the steady state of the actin-activated Mg^{2+}-ATPase, provided a sufficiently high concentration of ATP is used.

To examine whether prodan affects the interaction between actin and S-1, the actin-activated Mg^{2+}-ATPase of S-1 was studied in the presence and absence of prodan. The results were analyzed by a double-reciprocal plot of the ATPase rate against actin concentrations. In the absence of prodan, the ATPase rates, k_{cat}, were determined from P_i assays. In the presence of the probe, a rate constant (k_2), obtained from the decay curve of fluorescence, was taken as an actin-activated ATPase rate as described above (Table 1).

As shown in Figure 7b, the linear regression analyses of the data were carried out in the presence and absence of 4 μM prodan. The V_{max} value for S-1 (10 s^{-1}) was scarcely altered by prodan, yielding a value of 9.1 s^{-1} in the presence of the probe. This was also the case for the K_m value for actin. The value of 37 μM obtained in the presence of prodan was similar to that (35 μM) obtained in its absence. These results suggest that the addition of prodan to acto-S-1 scarcely interferes with the binding of actin to S-1, confirming the applicability of prodan to the direct measurements of the actin-activated Mg^{2+}-ATPase rates of S-1. Thus, these results have proven that prodan is extremely useful not only in the direct measurement of myosin ATPase rates but also in studies on the interaction between actin and S-1 since the probe is able to monitor the actin-activated ATPase reaction without interfering with the binding of actin to S-1.

Effect of the Base of NTP on Changes in Prodan Fluorescence. The results described above suggest that the prodan bound to S-1 senses differences in various conformational states of S-1 which are characterized by the S-1, S-1*·ADP, and S-1**·ADP·P_i states. To lend further support to this hypothesis, I next examined the ability of various NTPs to induce changes in prodan fluorescence.

Upon addition of various NTPs to the prodan·S-1 complex, the emission maximum of prodan was blue-shifted to 445 nm, regardless of its base structure (Figure 8a). However, the extent of enhancement of prodan fluorescence strongly depends on the base structure of NTP. The fluorescence was most effectively enhanced by the natural substrate ATP, with the effectiveness of other NTPs ordered as follows: ATP > CTP > UTP ≫ ITP > GTP. GTP was the least effective with an effectiveness of about 15% of that obtained with ATP. Interestingly, these data correlate well with the effectiveness of NTPs in supporting force production in muscle fibers (*27*, *28*) (Figure 8b). I also found that the order follows that of the extent of fluorescence enhancement of the Mant fluorophore attached to the corresponding NDPs in the S-1·NDP·V_i complexes (*29*) (Figure 8c). These correlations indicate that the prodan binding site on S-1 senses the biologically significant conformational changes which occur in the myosin head during NTP hydrolysis.

Effect of the Nucleotide Base on the Formation of S-1·NDP·V_i Complexes and NTP Hydrolysis. Taking advantage of a large nucleotide-induced change of prodan fluorescence, I also measured the rate constants for the formation of S-1·-

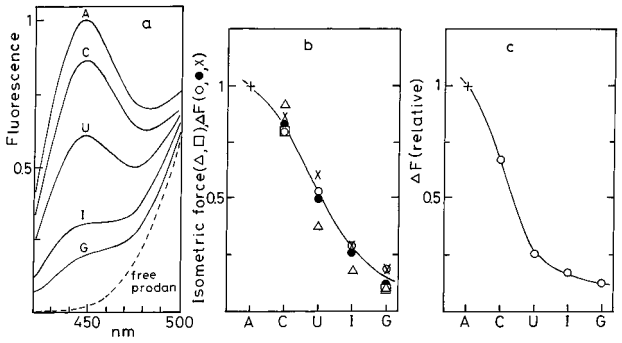

FIGURE 8: NTP-induced fluorescence enhancement of the S-1·prodan complex and its correlation with the NTP-produced force in muscle fibers and fluorescence enhancement of the Mant fluorophore attached to NDP trapped to S-1 with V_i. (a) Fluorescence spectra of prodan (1 μM) were measured in the presence of S-1 (9.8 μM) and NTP (4 mM) during NTP hydrolysis as described in Figure 1a. (b) Measured NTP-induced fluorescence enhancement was plotted as a function of the base structure of NTP: (×) 9.8 μM S-1, 4 mM NTP, and 1 μM prodan; (●) 9.8 μM S-1, 0.2 mM NTP, and 4 μM prodan; and (○) 1.2 μM S-1, 0.12 mM NTP, and 4 μM prodan. (△ and □) NTP-produced forces in muscle fibers, taken from Regnier et al. (*27*) and Pate et al. (*28*), respectively, were plotted as a function of the base structure of NTP. (c) The extent of enhancement in the Mant fluorescence of S-1·Mant-NDP·V_i complexes, taken from Hiratsuka (*29*), was plotted as a function of the base structure of Mant-NDP. All values are expressed relative to the values obtained with ATP (b) and Mant-ADP (c). A, C, U, I, and G indicate ATP, CTP, UTP, ITP, and GTP, respectively (a and b), and the corresponding Mant-NDPs (c).

NDP·V_i complexes and the initial velocities of the steady state of NTPases.

For all S-1·NDP complexes in the presence of prodan, the addition of V_i (0.2 mM) resulted in a fluorescence increase similar to that of the S-1·ADP complex (not shown). The resultant emission spectrum exhibited the same maximum at 445 nm for all complexes, regardless of its base structure. Rate constants for the formation of the complexes were calculated from an increase in prodan fluorescence as described in Figure 2b. The rate depended on the base structure of NDP and followed again the order ADP > CDP > UDP > IDP > GDP. The complex was most rapidly formed by the natural product ADP with a rate constant of 8.3×10^{-3} s^{-1}, whereas GDP was the least effective with a rate constant of 4.0×10^{-3} s^{-1}. The value for the ADP complex was very similar to that (7×10^{-3} s^{-1}) obtained from fluorescence changes of a covalent probe attached to Cys-707 of S-1 under a similar condition (30).

On the other hand, the initial velocities of NTPases were also measured from changes in fluorescence of prodan using various NTPs as substrates (not shown). GTP was hydrolyzed about 14 times (0.78 s^{-1}) faster than ATP, while ATP and CTP were hydrolyzed with a similar rate. The hydrolysis rate followed the order GTP > ITP > UTP $\gg$ CTP $\geq$ ATP. These data are essentially consistent with those reported by other investigators (*31*−*33*).

DISCUSSION

The X-ray crystallographic structure of S-1 reveals some clefts and pockets on the protein (*10*). The presence of a hydrophobic pocket on S-1 where various noncovalent fluorophores stoichiometrically bind was proposed some time ago (*11*). It has been shown that fluorescent probes ANS and its dimer bisANS bind stoichiometrically to myosin (*6*) and S-1 (*7*), respectively. However, the precise location of the binding sites of these probes on S-1 remains to be determined. This is also the case for the prodan binding site, although these results suggest that it includes none of the binding sites of ATP and actin. Taking into account the fact that either prodan or ANS bears the aminonaphthalene ring as a common structural unit, it is highly likely that both probes bind to the same hydrophobic pocket on S-1. This speculation is supported by the fact that the features of binding of ANS (*6*) and prodan to myosin and S-1 are similar, indicating the same stoichiometry of 1:1 and similar dissociation constants of 49 and 44 μM, respectively.

Recently, many efforts have been made to detect changes in hydrophobic sites on S-1 that are associated with the conformational changes in the ATP binding pocket during ATP hydrolysis. If hydrophobic interactions of nonpolar groups in S-1 were indeed involved in the energy transduction system of actomyosin, the conformational changes that occur in the ATP binding pocket might be sensed in hydrophobic sites on S-1. It has been found from measurements using hydrophobic chromatography that the hydrophobicity of S-1 is sensitive to the conformational states of the ATP binding pocket (*34*). A noncovalent hydrophobic fluorescent dye bound to S-1 has also been used to detect the conformational changes in a hydrophobic pocket that are associated with the ATP hydrolysis reaction (*20*).

Like the vast majority of the more commonly used fluorescent probes such as aminonaphthalenes (*1*), the emission maximum of prodan is dependent primarily on the dielectric constant of the solvent (*12*, *13*). When prodan is bound to S-1, its emission maximum is blue-shifted from 520 to 460 nm. The resultant blue fluorescence is extremely sensitive to the nucleotide-induced conformational states of S-1. Thus, the emission maximum is further blue-shifted to 450 nm upon binding to S-1 in the S-1*·ADP state. When the probe binds to S-1 during ATP hydrolysis, where S-1 is primarily in the S-1**·ADP·P_i state, not only is the emission maximum blue-shifted to 445 nm but the intensity is also enhanced about 4.5-fold. Thus, the prodan binding site on S-1 seems to be more hydrophobic during ATP hydrolysis. This explanation would be in accord with the recent result of Gopal and Burke (*34*), who showed using hydrophobic chromatography that the extent of hydrophobicity of S-1 is significantly altered upon addition of ATP. This work confirms the existence of such a site on S-1 which senses differences in the nucleotide-induced conformational states of S-1 (*6*, *7*, *20*).

Taking advantage of the ATP-induced change in absorption of an intrinsic chromophore of S-1, i.e., the indole ring of Trp, Morita could conveniently calculate the initial velocities of the steady state of the Mg^{2+}-ATPase of heavy meromyosin (*22*). This is also the case for the ATP-induced change in prodan fluorescence in this study. The data show that prodan binds to S-1 with a stoichiometry of 1:1 without affecting significantly the ATPase and actin-binding properties of S-1. Furthermore, neither ATP nor actin interferes with the prodan binding. These properties of prodan make the probe bound to S-1 behave like an intrinsic fluorophore of S-1, although the binding is noncovalent. Thus, properties of interaction between S-1 and nucleotides are evaluated from kinetic and equilibrium data without considering interaction

between S-1 and prodan. Indeed, an observed ATP-induced change, ΔF, of the fluorescence intensity at 445 nm was proportional to the concentration of a nucleotide·S-1 complex in this system. Therefore, considerations similar to those used in dealing with the ATP-induced change in absorbance of Trp residues of heavy meromyosin can be applied (*22*).

A similar application of a noncovalent fluorescent probe to kinetic studies of enzyme has been reported with another aminonaphthalene TNS for Ile-tRNA synthetase (*2*, *9*). The probe binds reversibly to the enzyme with a stoichiometry of 1:1 and a dissociation constant of 70 μM. This dissociation constant is 1.6 times greater than that (44 μM) for the prodan·S-1 complex. Binding of TNS to the enzyme interferes with neither substrate binding nor the enzyme action. Furthermore, the stoichiometry of TNS binding and the dissociation constant for the TNS·enzyme complex are scarcely altered by various substrates. Thus, TNS also behaves like an intrinsic fluorophore for the enzyme as well as prodan for S-1. Taking advantage of a large change in TNS fluorescence upon addition of various substrates to the enzyme, measurements of dissociation constants for the complexes of enzyme with various substrates (*2*) and preequilibrium kinetic studies using stopped-flow techniques (*9*) have successfully been performed.

In this paper, it has been demonstrated that initial velocities of the steady state of the ATPases by S-1 in the presence of not only Mg^{2+} but also Ca^{2+} can be conveniently calculated from the change in prodan fluorescence. Since prodan scarcely affects the binding of actin to S-1, this method can also be applied to measure the actin-activated Mg^{2+}-ATPase rate. The values obtained in concentration ranges from 0.5 to 11 μM and from 0.01 to 2.4 mM for S-1 and ATP, respectively, were essentially identical to those obtained from P_i assays. The technique is straightforward and simple to use and requires only a very small amount of S-1, provided a molar excess of ATP over S-1 of at least 18-fold is used. This method can easily be extended to investigate the properties of various NTPs as substrates for the myosin ATPase. The order of NTPase rates obtained from changes in prodan fluorescence essentially agrees with those of NTPase rates obtained by conventional methods for myosin and S-1 (*31*−*33*). Furthermore, the ability of different NTPs to enhance the prodan fluorescence gives a good indication of their ability to support force production in muscle fibers. Therefore, this method should greatly facilitate further studies of the ATPase mechanism especially for various myosins other than the myosins-II (*35*) since only small amounts of samples are available in such cases.

The use of prodan fluorescence is very suitable for monitoring the nucleotide-induced conformational changes of S-1, especially in the presence of V_i. Monitoring a slow process such as the formation of the stable ternary complex of S-1·ADP·V_i requires stability against photodegradation to allow data to be collected for long times. The proportional characters of the curves shown in Figure 5 (panels b and c) indicate that the prodan fluorophore in the S-1**·ADP·P_i state is stable for more than 25 min. Indeed, control experiments in the absence of protein indicate that virtually no photobleaching of the prodan fluorophore occurred over the 1 h period upon excitation at 360 nm. On the other hand, Trp fluorescence is not applicable to monitoring the formation of the S-1·ADP·V_i complex since the absorption of V_i in the UV regions interferes with the measurements (*16*). Furthermore, not only the fluorophore of Trp but also S-1 itself is susceptible to photodamage upon such a prolonged irradiation at 290 nm. Thus, the properties with negligible photodegradation and its excitation wavelength of 360 nm make prodan ideal for monitoring slow processes concerning the ADP·V_i-induced conformational changes of S-1.

It has been reported that the addition of V_i to the myosin·ADP complex produces a stable ternary state which mimics the transient myosin−products intermediate of ATP hydrolysis (*25*). It is interesting to compare the structure of the myosin·ADP·V_i complex with that of the steady state intermediate of the ATPase pathway, myosin**·ADP·P_i. The recent X-ray crystallographic study with the *Dictyostelium* S-1 motor domain has revealed that the structure of S-1 complexed with ADP and V_i is similar to that of S-1 in the S-1**·ADP·P_i state (*36*). This work with prodan provides further information on the conformational analogy between S-1 in the S-1·ADP·V_i complex and that in the S-1**·ADP·P_i state. The emission maximum of prodan bound to the S-1·ADP complex is at 450 nm, which differs from that (445 nm) of the bound probe during ATP hydrolysis. However, upon addition of V_i, the maximum is blue-shifted to 445 nm. Thus, these results suggest that there is no significant difference in conformations between the two S-1s in the S-1·ADP·V_i complex and the steady state intermediate S-1**·ADP·P_i, at least with respect to the region near the bound prodan. This conclusion is in accordance with the recent observations and conclusions obtained from the similarity between the two S-1 states in the extent of hydrophobicity of S-1 (*34*), the pattern of thermal unfolding of S-1 (*37*), and the reactivity of Cys-707 against thiol reagents (*38*).

In conclusion, prodan is a very useful fluorescent probe for the myosin ATPase because the ATPase rates can be measured directly from the fluorescence change even in the presence of actin. This method can also be applied to the measurement of hydrolysis rates of various NTPs with different base structures. Furthermore, the nucleotide-induced changes in prodan fluorescence provide not only an index of force production in muscle fibers but also information on the structural changes which occur in the myosin head during NTP hydrolysis. These results also raise the possibility that the ATPase reactions may be visualized by prodan under a fluorescence microscope for the measurements of thin filament movement in motility assays.

ACKNOWLEDGMENT

I am grateful to Kyoko Nakamura for typing the manuscript.

REFERENCES

1. McClure, W. O., and Edelman, G. M. (1967) *Biochemistry 6*, 559−566.
2. Holler, E., Bennett, E. L., and Calvin, M. (1971) *Biochem. Biophys. Res. Commun. 45*, 409−415.
3. Wu, C.-W., and Wu, F. Y.-H. (1973) *Biochemistry 12*, 4349−4355.
4. Colvert, K. K., Mills, D. A., and Richter, M. L. (1992) *Biochemistry 31*, 3930−3935.
5. Ruvinov, S. B., Yang, X.-J., Parris, K. D., Banik, U., Ahmed, S. A., Miles, E. W., and Sackett, D. L. (1995) *J. Biol. Chem. 270*, 6357−6369.

6. Cheung, H. C., and Morales, M. F. (1969) *Biochemistry 8*, 2177−2182.
7. Takashi, R., Tonomura, Y., and Morales, M. F. (1977) *Proc. Natl. Acad. Sci. U.S.A. 74*, 2334−2338.
8. Shi, L., Palleros, D. R., and Fink, A. L. (1994) *Biochemistry 33*, 7536−7546.
9. Holler, E., and Calvin, M. (1972) *Biochemistry 11*, 3741−3752.
10. Rayment, I., Rypniewski, W. R., Schmidt-Bäse, K., Smith, R., Tomchick, D. R., Benning, M. M., Winkelmann, D. A., Wesenberg, G., and Holden, H. M. (1993) *Science 261*, 50−58.
11. Haugland, R. P. (1975) *J. Supramol. Struct. 3*, 338−347.
12. Weber, G., and Farris, F. J. (1979) *Biochemistry 18*, 3075−3078.
13. Macgregor, R. B., and Weber, G. (1986) *Nature 319*, 70−73.
14. Mazumdar, M., Parrack, P. K., and Bhattacharyya, B. (1992) *Eur. J. Biochem. 204*, 127−132.
15. Chakrabarti, A. (1996) *Biochem. Biophys. Res. Commun. 226*, 495−497.
16. Goodno, C. C. (1979) *Proc. Natl. Acad. Sci. U.S.A. 76*, 2620−2624.
17. Weeds, A. G., and Taylor, R. S. (1975) *Nature 257*, 54−56.
18. Spudich, J. A., and Watt, S. (1971) *J. Biol. Chem. 246*, 4866−4871.
19. Hiratsuka, T. (1990) *J. Biol. Chem. 265*, 18786−18790.
20. Hiratsuka, T. (1994) *J. Biol. Chem. 269*, 27251−27257.
21. Fiske, C. H., and SubbaRow, Y. (1925) *J. Biol. Chem. 66*, 375−400.
22. Morita, F. (1967) *J. Biol. Chem. 242*, 4501−4506.
23. Chance, B. (1957) *Arch. Biochem. Biophys. 71*, 130−136.
24. Werber, M., Szent-Györgyi, A., and Fasman, G. (1972) *Biochemistry 11*, 2872−2883.
25. Goodno, C. C., and Taylor, E. W. (1982) *Proc. Natl. Acad. Sci. U.S.A. 79*, 21−25.
26. Hiromi, K., Ohnishi, M., and Yamashita, T. (1974) *J. Biochem. 76*, 1365−1367.
27. Regnier, M., Bostani, P., and Homsher, E. (1993) *Biophys. J. 64*, A250.
28. Pate, E., Franks-Skiba, K., White, H., and Cooke, R. (1993) *J. Biol. Chem. 268*, 10046−10053.
29. Hiratsuka, T. (1984) *J. Biochem. (Tokyo) 96*, 155−162.
30. Aguirre, R., Gonsoulin, F., and Cheung, H. C. (1986) *Biochemistry 25*, 6827−6835.
31. Weber, A. (1969) *J. Gen. Physiol. 53*, 781−791.
32. Seidel, J. C. (1975) *J. Biol. Chem. 250*, 5681−5687.
33. Eccleston, J. F., and Trentham, D. R. (1979) *Biochemistry 18*, 2896−2904.
34. Gopal, D., and Burke, M. (1996) *Biochemistry 35*, 506−512.
35. Cheney, R. E., Riley, M. A., and Mooseker, M. S. (1993) *Cell Motil. Cytoskeleton 24*, 215−223.
36. Smith, C. A., and Rayment, I. (1996) *Biochemistry 35*, 5404−5417.
37. Bobkov, A. A., and Levitsky, D. I. (1995) *Biochemistry 34*, 9708−9713.
38. Phan, B. C., Peyser, Y. M., Reisler, E., and Muhlrad, A. (1997) *Eur. J. Biochem. 243*, 636−642.

BI973083D